



# A NUMERICAL SOLUTION ALGORITHM FOR A HEAT AND MASS TRANSFER MODEL OF A DESALINATION SYSTEM BASED ON PACKED-BED HUMIDIFICATION AND BUBBLE COLUMN DEHUMIDIFICATION

Karim M. Chehayeb,<sup>1</sup> Farah K. Cheaib,<sup>2</sup> John H. Lienhard V<sup>1,\*</sup>

<sup>1</sup>Department of Mechanical Engineering, Massachusetts Institute of Technology, Cambridge, MA  
02139, USA

<sup>2</sup>Department of Mechanical Engineering, American University of Beirut, Beirut, Lebanon

## ABSTRACT

The humidification-dehumidification (HDH) desalination system can be advantageous in small-scale, off-grid applications. The main drawback of this technology has been its low energy efficiency, which results in high water production costs. Previous studies have approached this issue through thermodynamic balancing of the system; however, most theoretical work on the balancing of HDH has followed a fixed-effectiveness approach that does not explicitly consider transport processes in the components. Fixing the effectiveness of the heat and mass exchangers allows them to be modeled without explicitly sizing the components and gives insight on how the cycle design can be improved. However, linking the findings of fixed-effectiveness models to actual systems can be challenging, as the performance of the components depends mainly on the available surface areas and the flow rates of the air and water streams. In this study, we present a robust numerical solution algorithm for a heat and mass transfer model of a complete humidification-dehumidification system consisting of a packed-bed humidifier and a multi-tray bubble column dehumidifier. We look at the effect of varying the water-to-air mass flow rate ratio on the energy efficiency of the system, and we compare the results to those reached following a fixed-effectiveness approach. In addition, we study the effect of the top and bottom temperatures on the performance of the system. We recommended the implementation a control system that varies the mass flow rate ratio in order to keep the system balanced in off-design conditions, especially with varying top temperature.

**KEY WORDS:** Numerical simulation, energy efficiency, desalination, humidification, dehumidification, packed-bed, multi-tray, bubble column, thermodynamic balancing, heat and mass exchangers, HDH

## 1. INTRODUCTION

Humidification-dehumidification (HDH) is a technology which imitates the rain cycle in an engineered setting [1]. A typical cycle, shown in Fig. 1, consists of a humidifier, a dehumidifier, and a heater. Cold air enters the humidifier where it is put in direct contact with hot saline water, prompting evaporation of some of the water. The now hot and moist air is circulated through the dehumidifier where it is put in indirect contact with cold saline water flowing through tubing. This cools the humid air stream, causing some of its water vapor to condense, thus supplying a stream of fresh water.

The technology behind the operation of HDH systems is fairly simple, which makes the system robust and

\*Corresponding author: John H. Lienhard V: [lienhard@mit.edu](mailto:lienhard@mit.edu)

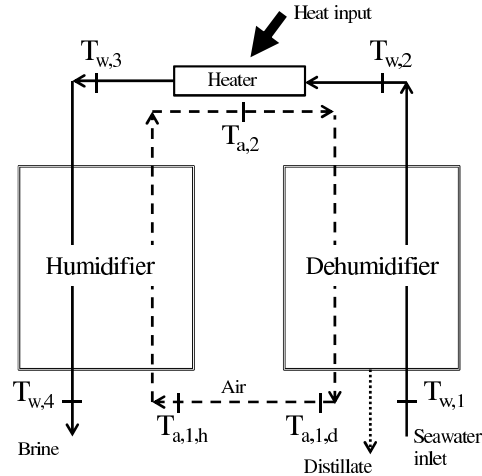


**Fig. 1** Schematic diagram representing an HDH system. Note that temperature labels are only used to explain the solution algorithm, and there is only one value of the air bottom temperature:  $T_{a,1} = T_{a,1,d} = T_{a,1,h}$ .

easy to operate compared to other desalination technologies. In addition, this technology can be competitive in small-scale, off-grid applications where the need for fresh water is not high enough to warrant the installation of large conventional thermal desalination plants, namely Multi-Stage Flash (MSF) and Multi-Effect Distillation (MED). Furthermore, HDH can tolerate much higher salinities than membrane-based desalination technologies, such as Reverse Osmosis (RO), which makes it suitable for treating produced water from hydraulically fractured oil and gas wells. However, the major drawback of this technology has been its low energy efficiency, which has prompted researchers to study the thermodynamics of the cycle, and to pinpoint the major causes of entropy generation.

Narayan et al. [2, 3] found that entropy generation within a system is minimized when the modified heat capacity rates of the air and water streams are equal in the dehumidifier. In addition, Narayan et al. [4], and Chehayeb et al. [5], used a fixed-effectiveness approach to model the thermodynamic balancing of HDH systems through mass extractions and injections. Fixing the effectiveness allows the determination of the performance of a heat and mass exchanger without the need for a specific transport model or for the specification of system dimensions. While this approach is useful in understanding the thermodynamics of the HDH system, its results can be difficult to translate into practical design, which motivates the current work on establishing a numerical heat and mass transfer model of a complete HDH system.

In this study, we present a robust numerical solution algorithm for a transport model of a humidification-dehumidification desalination system consisting of a packed-bed humidifier and a multi-tray bubble column dehumidifier. We look at the effect of varying the water-to-air mass flow rate ratio on the performance of the system. In addition, we study the effect of the top and bottom temperatures in an attempt to model operation under variable conditions. The importance of this robust solution method lies in its ability to model different configurations of the HDH desalination system, including the variation of the mass flow rate ratio through extractions and injections of either air or water, which would be impossible to achieve by using a simple simultaneous equation solver.

## 2. MODELING

Establishing an accurate model of a complete humidification-dehumidification system allows us to simulate the effect of various parameters with significant practical importance. In addition, implementing models of the basic components of the system in MATLAB allows flexibility in varying the conditions of operation, and

also allows us to model different configurations of these components. This section presents the models of the different components of the HDH system, and the algorithms used to solve them.

## 2.1 Bubble column dehumidifier

The use of a short bubble column for dehumidification was first introduced by Narayan et al. [6] and was found to be very promising since it reduces the negative effect of the noncondensable gases on condensation. In traditional dehumidification systems, water vapor has to diffuse through an air layer, which increases the resistance to the mass transfer. In a bubble column, the location of condensation is the transiently formed bubble-water interface which has a very large specific area, giving it superior efficiency compared to alternative dehumidification systems [6, 7].

In a bubble column dehumidifier, cold saline water and hot moist air exchange heat and mass through a stationary column of fresh water. The saline water is circulated through a coil immersed in the column of fresh water, and the hot humid air is bubbled from the bottom of the column through a sparger. As the air passes through the column, it is cooled and dehumidified.

*2.1.1 Governing equations* This study uses the model established by Tow and Lienhard [7–9] to evaluate the performance of the dehumidifier bubble column. This model is based on a resistance network between the hot air and cold saline water. To further simplify the resistance model, Tow assumes perfect mixing in the column, meaning that the air always exits the dehumidifier at the column temperature, and that the air side resistance to heat and mass transfer is negligible, leaving the model with just two resistances to the transfer of heat from the column to the cold saline water. The outer resistance,  $R_o$ , is between the column and the coil, and the inner resistance,  $R_i$ , is between the coil and the saline water. Tow's model relies on well established models to describe these resistances, and has been verified experimentally for various conditions.

For generality, and to be able to use the model in a multi-tray dehumidifier, we assume that some fresh water also enters the column. Performing a water mass balance on the system allows us to calculate the mass flow rate of the condensate leaving the column:

$$\dot{m}_{\text{cond,out}} = \dot{m}_{\text{cond,in}} + \dot{m}_{\text{da}} (\omega_{\text{in}} - \omega_{\text{out}}) \quad (1)$$

Note that the condensate will be bled from the column (at the column temperature) in order to keep the process running at steady state. In addition, the energy balance can be written as

$$\dot{m}_{\text{da}} (h_{\text{a,in}} - h_{\text{a,out}}) + \dot{m}_{\text{cond,in}} h_{\text{cond,in}} - \dot{m}_{\text{cond,out}} h_{\text{cond,out}} = \dot{m}_{\text{w}} (h_{\text{w,out}} - h_{\text{w,in}}) \equiv \dot{Q}_1 \quad (2)$$

We denote this quantity as  $\dot{Q}_1$  for clarity in the solution method. A logarithmic mean temperature difference is defined since the saline water exchanges heat with the column that is at fixed temperature

$$\Delta T_{\text{lm}} = \frac{T_{\text{w,out}} - T_{\text{w,in}}}{\ln \left( \frac{T_{\text{col}} - T_{\text{w,in}}}{T_{\text{col}} - T_{\text{w,out}}} \right)} \quad (3)$$

And the heat transfer to the saline water can be expressed as

$$\dot{Q}_2 = \frac{\Delta T_{\text{lm}}}{R_{\text{in}} + R_{\text{out}}} \quad (4)$$

We note that performing an energy balance on the saline water implies that  $\dot{Q}_1 = \dot{Q}_2$ , and the only reason these two quantities are denoted differently is to clarify the solution method.

*2.1.2 Solution method* The equations governing the bubble column dehumidifier are nonlinear due to the presence of the logarithmic mean temperature difference. This section presents a method to solve these nonlinear

equations in a linear manner using a computer program such as MATLAB. In a typical single-tray bubble column dehumidifier, the inlet temperatures are specified. However, when simulating the multi-tray bubble column, described in Section 2.2, two other cases arise.

*Case 1* This case is encountered when we are studying a single-tray bubble column where the flow rates and the inlet temperatures are specified. The detailed algorithm for the solution method is presented in Fig. A.9, but a basic description of the approach will be presented here. The first step in the solution method is to guess the air outlet temperature using the bisection method. We know from the model that both the air and the condensate exit at the column temperature, so the only unknown left in this problem is the water outlet temperature, which can be calculated using Eq. 2. Next, the heat transfer that is governed by the size of the system,  $\dot{Q}_2$ , can be calculated using Eq. 4. The guessed value of  $T_{a,out}$  is modified depending on the calculated values of  $\dot{Q}_1$  and  $\dot{Q}_2$ , as explained in Fig. A.9.

*Case 2* The importance of Cases 2 and 3 will be apparent in Section 2.2. We denote by Case 2 the dehumidifier in which the air inlet temperature and the water outlet temperature are specified. This can be thought of as solving for the cold end of the system given the conditions at the hot end. The solution method for this case is almost identical to Case 1, the only difference being the use of Eq. 2 to calculate  $T_{w,in}$  instead of  $T_{w,out}$ .

*Case 3* We denote by Case 3 the system in which  $T_{a,out}$  and  $T_{w,in}$  are specified. In other words, we are interested in determining the temperatures at the hot end of the system, given the conditions at the cold end. The solution method in this case is similar to Cases 1 and 2, but, instead of guessing  $T_{a,out}$ , we guess the value of  $T_{w,out}$  and then calculate  $\dot{Q}_1$  using Eq. 2 and  $\dot{Q}_2$  using Eq. 4. From there, the calculation proceeds according to Fig. A.9. When the guessed values of  $T_{w,out}$  converge, and we have  $\dot{Q}_1 = \dot{Q}_2$ , we can calculate  $T_{a,in}$  from Eq. 2.

## 2.2 Multi-tray bubble column dehumidifier

One drawback to the use of a bubble column is that even though the water and air streams flow in a counterflow manner, both streams interact with the fresh water in the column which is at constant temperature. This means that, even at infinite coil length, the saline water will only reach the air outlet temperature. Tow discusses this phenomenon in detail before defining a parallel flow effectiveness as the appropriate performance metric [7]. However, the height of a single-tray bubble column can be made very small, and multiple trays, each at a different temperature, can be stacked to form a multi-tray bubble column which is no longer limited to the performance of a parallel flow device, as shown in Fig. 2, where the temperature profiles are plotted against the normalized enthalpy, which is the change in enthalpy from the cold end over the total enthalpy change.

The governing equations for a multi-tray bubble column are the equations of a single tray, discussed in Section 2.1, repeated for each tray, with additional equations for matching the boundary conditions between consecutive trays. One issue that makes solving these equations challenging is that the temperatures of water and air between the trays are unknown, as only the inlet temperatures are given. The system, therefore, has to be solved numerically. This is done by guessing one of the outlet temperatures and constructing the temperature profiles up to the other end by using the dehumidifier functions (Cases 2 and 3). The calculated inlet temperature is then compared to the specified value, and the guessed value is changed accordingly, as shown in detail in Fig. A.10.

In some cases, when the available coil area is large, high effectiveness makes the numerical analysis fail if the temperature is guessed at the wrong end. In order to explain this issue better, we first consider the modified heat capacity rate ratio (HCR) defined by Narayan et al. [2] as follows:

$$\text{HCR} = \frac{\Delta \dot{H}_{\max, \text{cold}}}{\Delta \dot{H}_{\max, \text{hot}}} \quad (5)$$

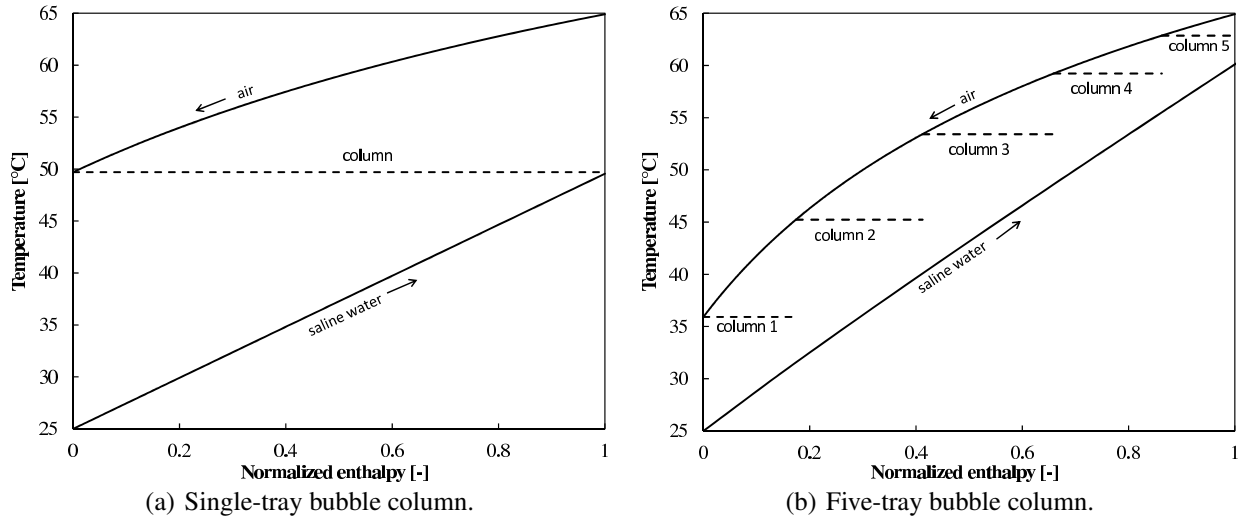


**Fig. 2** Comparison of the performance of a single-tray bubble column and a five-tray bubble column. Both dehumidifiers have the same size, and operate under the same conditions. In the multi-tray dehumidifier, the coil length is divided equally between the trays.

In the case of a multi-tray bubble column dehumidifier with no inflow of condensate, the cold stream consists of the saline feed water, and the hot stream consists of the moist air and the condensing fresh water stream. The modified heat capacity rate ratio can therefore be expressed as:

$$\text{HCR}_d = \frac{\dot{m}_w (h_w|_{T_{a,\text{in}}} - h_w|_{T_{w,\text{in}}})}{\dot{m}_{\text{da}} (h_a|_{T_{a,\text{in}}} - h_a|_{T_{w,\text{in}}}) - \dot{m}_{\text{da}} (\omega|_{T_{a,\text{in}}} - \omega|_{T_{w,\text{in}}}) h_{\text{cond}}|_{T_{w,\text{in}}}} \quad (6)$$

When the area of the system is large enough to get a high effectiveness, and  $\text{HCR}_d$  is greater than unity, the air stream, having a lower heat capacity rate, will exit the heat and mass exchanger at a temperature close to the inlet temperature of the saline water. In addition, at the cold end of the system, the temperature variation will become very small since the driving force of the heat and mass exchange is small. This means that a small change in  $T_{a,\text{out}}$  will result in a large change of the temperature profile on the hot side. This problem is resolved by building the profile starting from the hot side, so that  $T_{w,\text{out}}$  is guessed. Depending upon the calculated value of  $T_{w,\text{in}}$ , a new  $T_{w,\text{out}}$  guess value is picked, as explained in detail in Fig. A.10.

## 2.3 Packed-bed humidifier

The packed-bed humidifier in an HDH system is essentially the same as a cooling tower used in a power plant, but with the purpose of humidifying the air stream. Thanks to the widespread use of cooling towers, the packed-bed humidifier can be modeled fairly accurately by using the most thorough model for cooling towers, namely the Poppe and Rögener model [10]. Kloppers and Kröger [11] have published a detailed algorithm to solve the equations of the model numerically using the fourth order Runge-Kutta method. The rest of this section briefly describes the governing equations for heat and mass transfer in the humidifier, and presents the algorithm used in finding their solution.

**2.3.1 Governing equations and solving method** As explained by Kloppers and Kröger [11], determining the performance of the humidifier involves solving for the four main variables: the water temperature,  $T_w$ , the enthalpy of moist air,  $h_a$ , the absolute humidity,  $\omega$ , and the Merkel number,  $\text{Me}$ , at different locations within the humidifier, where  $\text{Me}$  is a dimensionless parameter that captures the effect of the system size. The variation

**Table 1** Specifications of the system studied.

<b>Operating conditions</b>	
Top temperature, $T_{\text{top}}$	90 °C
Bottom temperature, $T_{\text{bottom}}$	25 °C
Feed mass flow rate, $\dot{m}_{w,\text{in}}$	0.242 kg/s
<b>Humidifier geometry</b>	
Height	3 m
Cross-sectional area	0.05 m <sup>2</sup>
Fill surface area	226 m <sup>2</sup> /m <sup>3</sup>
Merkel number, Me	$0.967 \left( \frac{\dot{m}_w}{\dot{m}_a} \right)^{-0.779} \times (3.28 H)^{0.632}$
Minimum-maximum water loading	13.4-32 m <sup>3</sup> /hr – m <sup>2</sup>
<b>Dehumidifier geometry</b>	
Pipe length per tray	2.5 m
Number of trays	30
Pipe outer/inner diameter	9.5 mm/8.7 mm
Coil diameter	0.4 m

of the four variables along the humidifier can be expressed in terms of the change in water temperature:

$$\frac{dh_a}{dT_w} = f_1(T_w, h_a, \omega, \text{Me}) \quad (7)$$

$$\frac{d\omega}{dT_w} = f_2(T_w, h_a, \omega, \text{Me}) \quad (8)$$

$$\frac{d\text{Me}}{dT_w} = f_3(T_w, h_a, \omega, \text{Me}) \quad (9)$$

where  $f_1$ ,  $f_2$ , and  $f_3$  are functions given by Kloppers and Kröger [11]. In order to determine the temperature profiles of air and water in the humidifier, these equations have to be solved numerically at small intervals. The algorithm is explained in Fig. A.8 in the Appendix, but some steps will be discussed here in greater detail. Given the water and air inlet temperatures, the first step is to guess the water outlet temperature using the bisection method. The humidifier is then divided into an appropriate number of intervals of constant water temperature change,  $\Delta T_w$ . These intervals serve as a basis of solving Eq. 7, 8, and 9. At the cold end, the temperatures are known, the air properties,  $h_a$  and  $\omega$ , are evaluated at saturation, and the Merkel number, Me, is set to 0. This gives us a complete set of boundary conditions at the cold end. Solving the differential equations numerically starting at the cold end allows us to build a complete profile up until the hot end where the boundary conditions are checked, and the procedure is repeated with an appropriate new guess value for the water inlet temperature, as explained in Fig. A.8. For further details on the solution method, and on cooling towers in general, the reader should refer to Klopper's doctoral thesis [12].

The specifications of the fill used in this analysis were adopted from Brentwood Industries (model number: CF-1200MA) and are summarized in Table 1.

## 2.4 Humidification-dehumidification system

The full HDH system consists of a packed bed humidifier and a multi-tray bubble column dehumidifier. The governing equations are those mentioned above for each component. In addition, as shown in Fig. 1, the air temperatures have to match between the humidifier and the dehumidifier. The solution method for the system can be thought of as analogous to the real system reaching steady state operation. Starting with the bottom air temperature,  $T_{a,1,h}$ , equal to the bottom temperature of the system, the humidifier function is called, and  $T_{a,2}$  is calculated. The obtained value of  $T_{a,2}$  is then input into the multi-tray dehumidifier function, which returns

a new value for  $T_{a,1,d}$ . If the error on  $T_{a,1}$  is higher than acceptable, the procedure is repeated with the new temperature until we get  $T_{a,1} = T_{a,1,d} = T_{a,1,h}$ .

## 2.5 Performance parameters

A widely used measure of the energy efficiency of a thermal desalination system is the Gained Output Ratio, GOR, defined as

$$\text{GOR} = \frac{\dot{m}_{pw} h_{fg}}{\dot{Q}_{in}} \quad (10)$$

GOR measures the degree of reuse of the heat input. A desalination system that does not recover the heat of condensation will have at most a GOR of 1, which is achieved if none of the heat is dissipated.

Another important measure of performance is the Recovery Ratio, RR, which is basically the ratio of fresh water to feed water:

$$\text{RR} = \frac{\dot{m}_{pw}}{\dot{m}_w} \quad (11)$$

## 3. RESULTS AND DISCUSSION

The specifications of the system presented in this section are summarized in Table 1. The superficial air velocity in the dehumidifier was fixed at 10 cm/s (a value known to be in the regime for which the model was developed), and the cross-sectional area of the bubble column was varied according to the definition of superficial velocity:

$$V_g = \frac{\dot{m}_a}{\rho_a A_{col}} \quad (12)$$

### 3.1 Effect of the heat capacity rate ratio on performance

The first step of this study was to make sure the results of this fixed-area model matched those generated by the fixed-effectiveness model suggested by Narayan et al. [2]. The effect of  $\text{HCR}_d$  (Eq. 5) on the performance of the system was studied in this section. Equation 6 shows that the value of  $\text{HCR}_d$  depends on the bottom temperature, the top air temperature,  $T_{a,2}$ , and the water-to-air mass flow rate ratio defined as

$$\text{MR} = \frac{\dot{m}_w}{\dot{m}_{da}} \quad (13)$$

Note that the top air temperature is not an input, but is rather determined by simulating the system, as explained in Section 2.4. In other words, the top air temperature depends on the top and bottom temperatures of the system, the mass flow rates of air and water, and the size of the system. For a system of fixed size, and given top and bottom temperatures, the value of  $\text{HCR}_d$  can be changed by varying the mass flow rate ratio.

As can be seen in Fig. 3(a), the GOR of a system with fixed area is maximized when  $\text{HCR}_d$  is equal to unity. In other words, the heat capacity rates of the interacting streams in the dehumidifier are equal. This result reiterates the importance of  $\text{HCR}_d$  in extracting the best performance from the HDH system.

Similarly, setting  $\text{HCR}_d$  to unity results in the highest possible recovery ratio, as shown in Fig. 3(b). The reason behind this behavior is that, when  $\text{HCR}_d = 1$ , the effectiveness is at a minimum for this system, which means that the driving force will not become too small at either end of the exchanger. This can be explained by considering an unbalanced system with a high effectiveness. Because the heat capacity rates of the streams are different, the stream with the smaller heat capacity rate will reach a temperature close to that of the other stream, and the driving force for the transport will become small for a portion of available area, resulting in only a small amount of heat and mass transfer in that portion. When  $\text{HCR}_d = 1$ , at any point in the heat

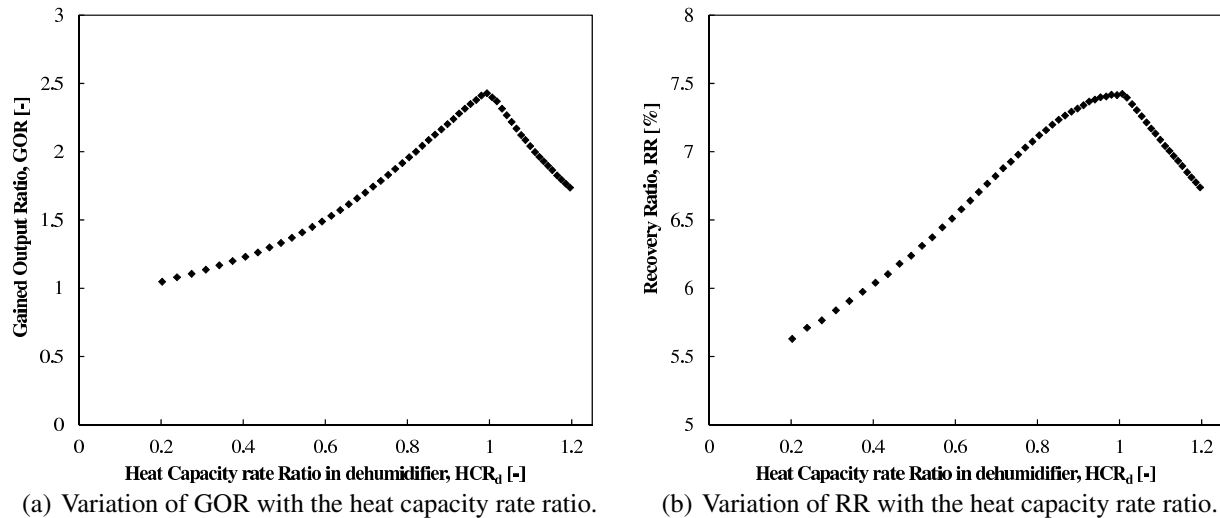


**Fig. 3** Effect of  $HCR_d$  on performance.

and mass exchanger there will be a finite driving force that will prompt the maximum possible heat and mass transfer. A high effectiveness is only desired when the system is balanced. It is a disadvantage to be limited by a small maximum heat duty, even if that value is reached.

### 3.2 Effect of bottom temperature on system performance

This section simulates the same system described in Table 1 except with a varying bottom temperature. This is done in order to evaluate the effect of a changing ambient water temperature.

**3.2.1 Variation of heat capacity rate ratio with bottom temperature** For a system designed to operate between  $25^\circ\text{C}$  and  $90^\circ\text{C}$ , it was shown in Section 3.1 that only one mass flow rate ratio ( $MR = 4.2$ ) results in a balanced system, and thus the best performance. If we fix the mass flow rate ratio to the design value of 4.2, it can be seen in Fig. 4 that  $HCR_d$  will change from unity as the bottom temperature deviates from the design value of  $25^\circ\text{C}$ , and the system will no longer be balanced, resulting in a drop in performance.

**3.2.2 Variation of mass flow rate ratio with bottom temperature** When the bottom temperature changes from the design value, bringing  $HCR_d$  back to unity would require changing the operating mass flow rate ratio. Figure 4 presents the optimal operating mass flow rate ratio for this system at any bottom temperature. It can be seen that, when the bottom temperature increases, the mass flow rate ratio should also be increased to keep the system balanced. This result can be explained by looking back at Eq. 6. However, we should note that even though the variation of  $HCR_d$  with the bottom temperature is linear, the same cannot be said about the variation of  $MR$  since  $HCR_d$  depends on the top air temperature which is also a function of the  $MR$ .

**3.2.3 Variation of GOR with bottom temperature** Figure 5(a) shows the variation of GOR with bottom temperature for two systems. The first system is designed to operate between  $25^\circ\text{C}$  and  $90^\circ\text{C}$ , meaning that its fixed  $MR$  only results in a balanced system at the design conditions. As the bottom temperature varies, as shown in Fig. 4,  $HCR_d$  will deviate from 1, and, as expected, GOR will drop. The other system allows for the variation of  $MR$  such that  $HCR_d$  is always equal to unity. We can see that the effect of increasing the bottom temperature while keeping  $HCR_d = 1$  is to raise GOR. This is expected since, for the same area, the water can reach a higher temperature before entering the heater, and therefore the required heat input will drop, and GOR will increase. Also, comparing the two curves in Fig. 5(a), we can see the importance of balancing on the energy efficiency of the HDH cycle. If the system is installed in a location where the temperature of the water



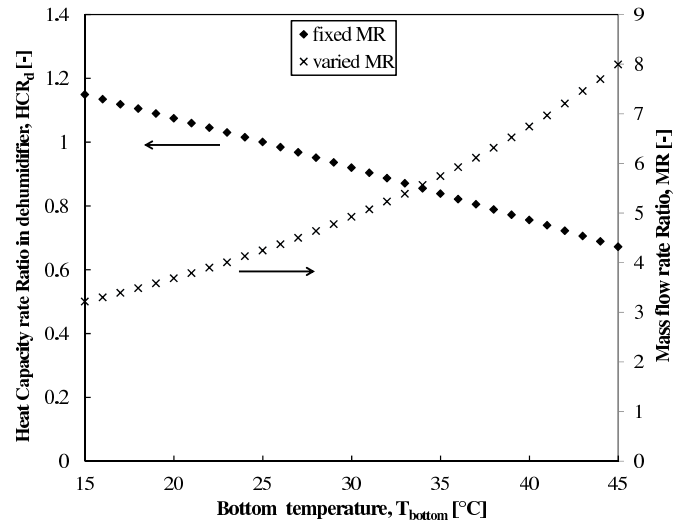


**Fig. 4** Variation of the  $HCR_d$  with bottom temperature for a system of fixed MR, and the variation of MR with bottom temperature for a system of  $HCR_d = 1$ .

to be treated fluctuates greatly, it could be economical to install a control system that would vary the flow rate of the air stream to meet the MR profile shown in Fig. 4 in order to keep  $HCR_d$  equal to unity.

3.2.4 Variation of RR with bottom temperature As can be seen in Fig. 5(b), the effect of balancing on RR is not as big as that on GOR. This observation indicates that the advantage of balancing is mainly to lower the heat input required to operate the system.

It is worth noting that satisfying  $HCR_d = 1$  will always maximize the output of the system, while also increasing the energy efficiency. For bottom temperatures higher than  $25^\circ\text{C}$ , the required MR, shown in Fig. 4, will be higher than in the unbalanced system, and the flow rate of air will be lower, but the system will still produce more water and at a higher energy efficiency. This result shows that adding more air to the system will not necessarily produce more water, and will not necessarily provide the water with more preheating. In fact, when the air flow rate is increased, the top air temperature will drop, so there is a possibility that the total amount of water produced will drop. Picking the correct flow rates is a balance between the humidifier and the dehumidifier, and it turns out that matching the heat capacity rates is the key in getting the best performance in terms of both, energy efficiency and productivity.

### 3.3 Effect of top temperature on system performance

This section discusses the effect of the top temperature, which can vary if the heat source of the system is not constant. A typical application would be solar heating, where the solar irradiation can vary greatly during the operation of the system. The system studied has the specifications described in Table 1 except that the top temperature is allowed to vary.

3.3.1 Variation of heat capacity rate ratio with top temperature Figure 6 shows the effect of the top temperature on  $HCR_d$  while keeping MR constant and equal to 4.2. We can see that, as the top temperature drops from the design value of  $90^\circ\text{C}$ ,  $HCR_d$  increases and deviates from unity, so we can expect the performance to drop.

3.3.2 Variation of mass flow rate ratio with top temperature It follows from Eq. 6 that we would need to decrease MR as the top temperature drops from the design value in order to keep  $HCR_d$  equal to unity. The optimal MR at various top temperatures is shown in Fig. 6. Similar to the optimal MR profiles presented in

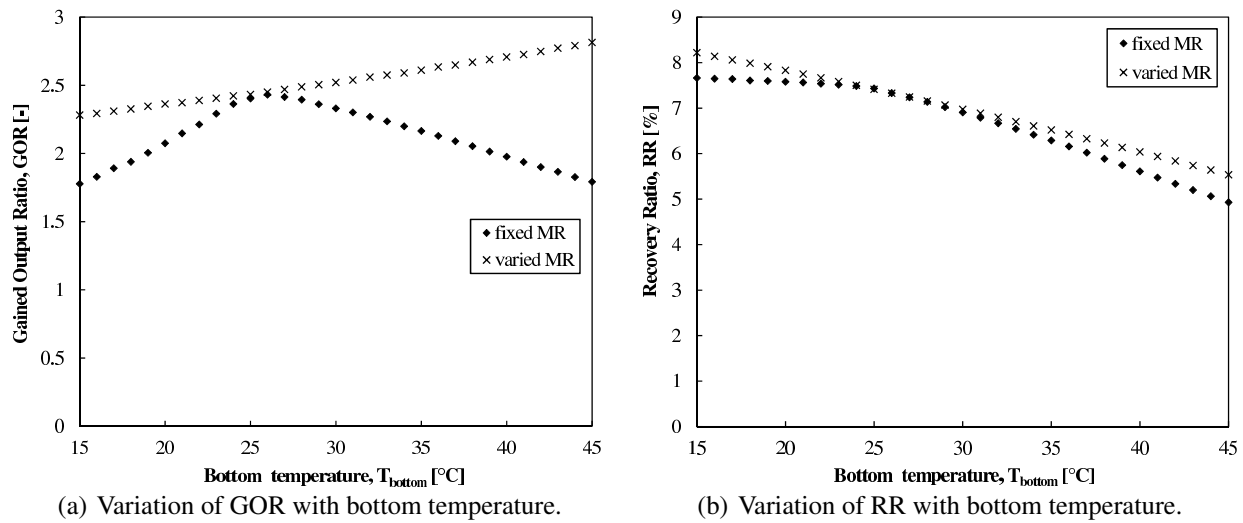


**Fig. 5** Effect of bottom temperature on performance.

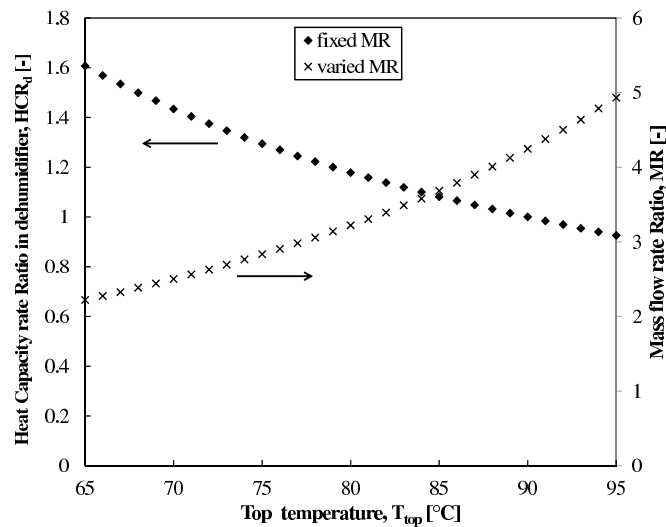


**Fig. 6** Variation of the  $HCR_d$  with top temperature for a system of fixed MR, and the variation of MR with top temperature for a system of fixed  $HCR_d = 1$ .

Fig. 4 and 6, we could generate all possible combinations of top and bottom temperatures of interest, and find the optimal MR at each of these pairs, which could be then input into the control unit of the system.

**3.3.3 Variation of GOR with top temperature** Figure 7(a) shows the variation of the GOR of two systems with the top temperature. The first system is designed to operate between 25 °C and 90 °C, so has  $MR = 4.2$  to get  $HCR_d = 1$  at 25 °C and 90 °C. But as the top temperature varies, MR is kept constant, so the performance of the system drops. The second system is a dynamic system that adjusts its MR such that  $HCR_d$  is always equal to unity. We can see that, when the top temperature drops, the energy efficiency of the dynamic system actually increases slightly.

The difference between the dynamic and passive systems in terms of GOR is quite significant, which indicates that if an HDH system relies on a heating source that is not constant, such as solar heating, the system should be flexible in adopting different mass flow rates of air to compensate for the change in top temperature. If a control system is not feasible, the system should be designed by taking into consideration the variation of the top temperature, and should operate at the MR that maximizes the total output over a certain period of time.

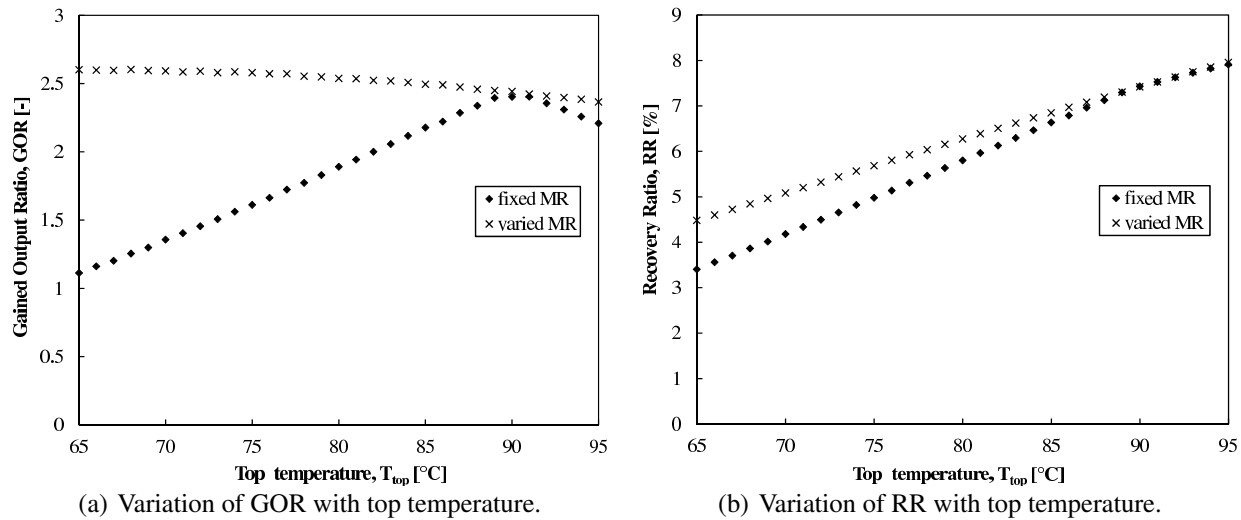


**Fig. 7** Effect of top temperature on performance.

**3.3.4 Variation of RR with top temperature** As shown in Fig. 7(b), the effect of the top temperature on the recovery is very large even if the system operates under variable MR. The reason behind this strong dependence is the exponential relation between absolute humidity and temperature. Operating the system at a higher temperature allows a large quantity of water to evaporate in the humidifier, and then condense in the dehumidifier, giving rise to a high recovery. Although balancing does not have a substantial effect on recovery, it should be noted that, as seen in Fig. 7(a), it does have a substantial effect on the energy efficiency of the system; in fact, it should be a strong enough effect to make it economical.

## 4. CONCLUSIONS

This study presents a robust solution algorithm for a transport model of a complete HDH system. The effects of operating in off-design conditions have been studied, and optimal mass flow rate ratios have been suggested for various top and bottom temperatures. The main conclusions drawn from this study are the following:

1. Thermodynamically balancing an HDH system, which is done by setting  $HCR_d = 1$ , maximizes energy efficiency and water recovery. It is therefore recommended to always operate at the mass flow rate ratio that results in  $HCR_d = 1$ .

2. It is recommended to implement a control system that varies the mass flow rate ratio in order to keep the system balanced in off-design conditions, especially with varying top temperature.
3. The effect of thermodynamic balancing is much larger on energy efficiency than on water recovery.
4. The effect of the top temperature on performance is much larger than that of the bottom temperature.

### ACKNOWLEDGMENTS

The authors would like to thank King Fahd University of Petroleum and Minerals for funding the research reported in this paper through the Center for Clean Water and Clean Energy at MIT and KFUPM (project # R4-CW-08).

### REFERENCES

- [1] G. P. Narayan and J. H. Lienhard V, “Humidification-dehumidification desalination,” in *Desalination: Water from Water*, Salem, MA: Scrivener Publishing, 2013.
- [2] G. P. Narayan, J. H. Lienhard V, and S. M. Zubair, “Entropy generation minimization of combined heat and mass transfer devices,” *International Journal of Thermal Sciences*, vol. 49, no. 10, pp. 2057 – 2066, 2010.
- [3] G. P. Narayan, K. H. Mistry, M. H. Sharqawy, S. M. Zubair, and J. H. Lienhard V, “Energy effectiveness of simultaneous heat and mass exchange devices,” *Frontiers in Heat and Mass Transfer*, vol. 1, no. 2, pp. 1–13, 2010.
- [4] G. P. Narayan, K. M. Chehayeb, R. K. McGovern, G. P. Thiel, S. M. Zubair, and J. H. Lienhard V, “Thermodynamic balancing of the humidification dehumidification desalination system by mass extraction and injection,” *International Journal of Heat and Mass Transfer*, vol. 57, pp. 756 – 770, 2013.
- [5] K. M. Chehayeb, G. Prakash Narayan, S. M. Zubair, and J. H. Lienhard V, “Use of multiple extractions and injections to thermodynamically balance the humidification dehumidification desalination system,” *International Journal of Heat and Mass Transfer*, vol. 68, pp. 422–434, 2014.
- [6] G. P. Narayan, M. H. Sharqawy, S. Lam, S. K. Das, and J. H. Lienhard V, “Bubble columns for condensation at high concentrations of noncondensable gas: Heat-transfer model and experiments,” *AIChE Journal*, vol. 59, no. 5, pp. 1780–1790, 2013.
- [7] E. W. Tow and J. H. Lienhard V, “Experiments and modeling of bubble column dehumidifier performance,” *International Journal of Thermal Sciences*, Submitted June 2013.
- [8] E. W. Tow and J. H. Lienhard V, “Analytical modeling of a bubble column dehumidifier,” in *Proceedings of the ASME 2013 Summer Heat Transfer Conference*, no. HT2013-17763, Minneapolis, MN, July 2013.
- [9] E. W. Tow and J. H. Lienhard V, “Heat flux and effectiveness in bubble column dehumidifiers for HDH desalination,” in *IDA World Congress on Desalination and Water Reuse*, Tianjin, China, October 2013.
- [10] M. Poppe and H. Rögener, “Berechnung von rückkühlwerken,” *VDI-Wärmeatlas*, vol. 111, pp. 1–15, 1991.
- [11] J. Kloppers and D. Kröger, “A critical investigation into the heat and mass transfer analysis of counterflow wet-cooling towers,” *International Journal of Heat and Mass Transfer*, vol. 48, no. 34, pp. 765 – 777, 2005.
- [12] J. C. Kloppers, *A critical evaluation and refinement of the performance prediction of wet-cooling towers*. PhD thesis, Stellenbosch: University of Stellenbosch, 2003.

Nomenclature, subscripts			
$a$	moist air	$da$	dry air
$col$	coolcolumn	$pw$	pure water
$cond$	condensate	$w$	seawater
$d$	dehumidifier		

## Appendix A. SOLUTION ALGORITHM FLOWCHARTS

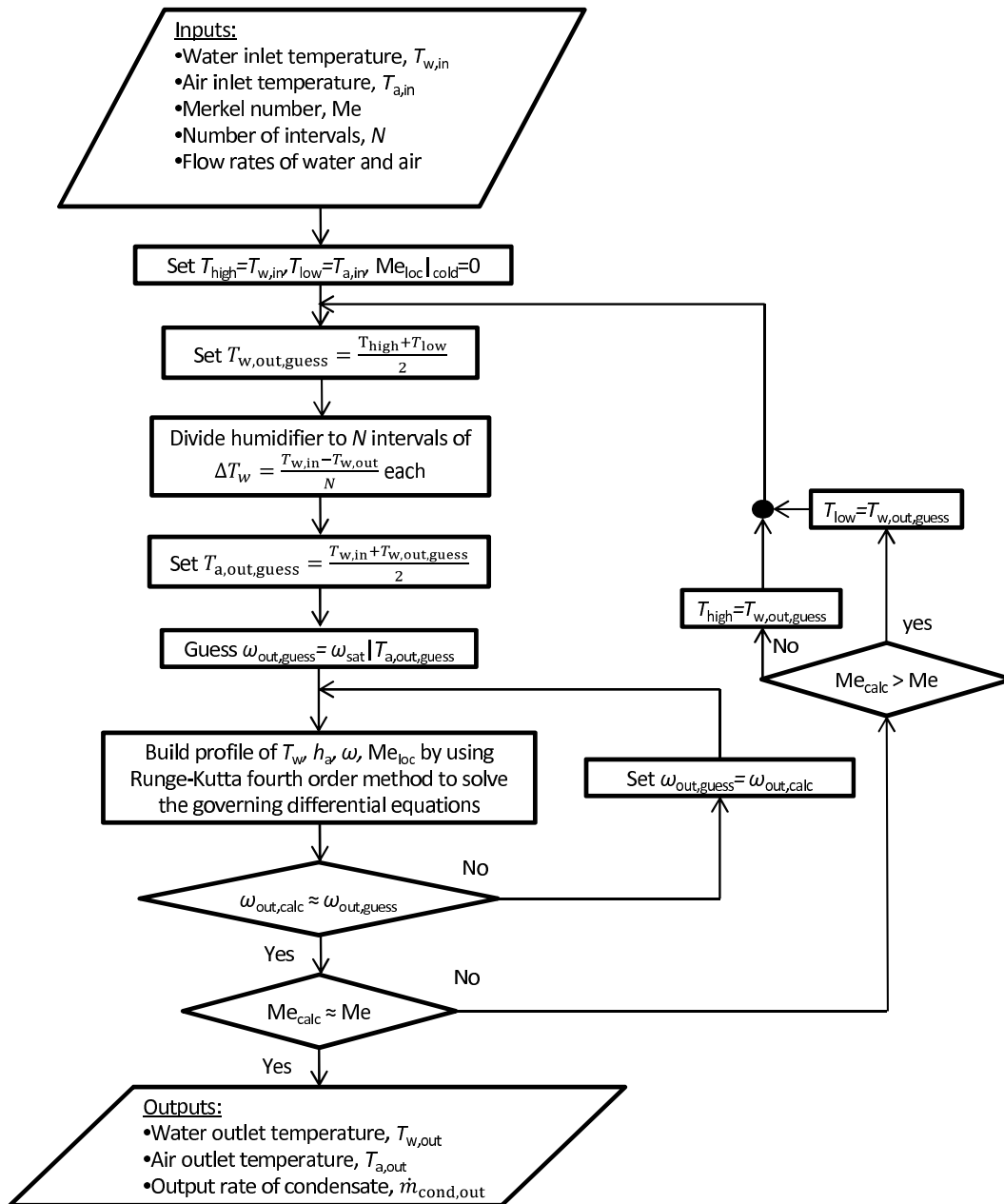


Fig. A.8 Solution algorithm for the packed-bed humidifier.

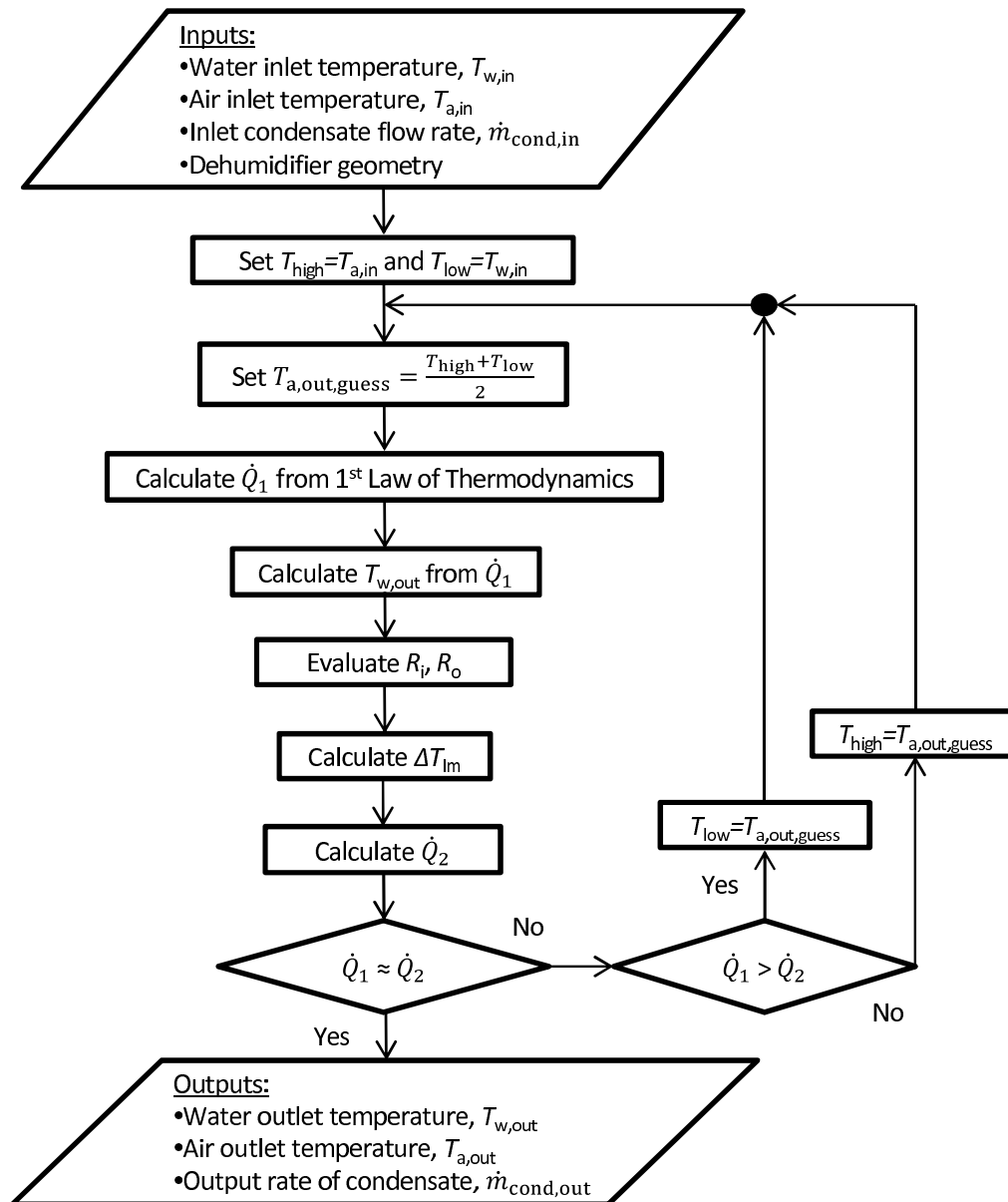


Fig. A.9 Solution algorithm for the bubble column dehumidifier.

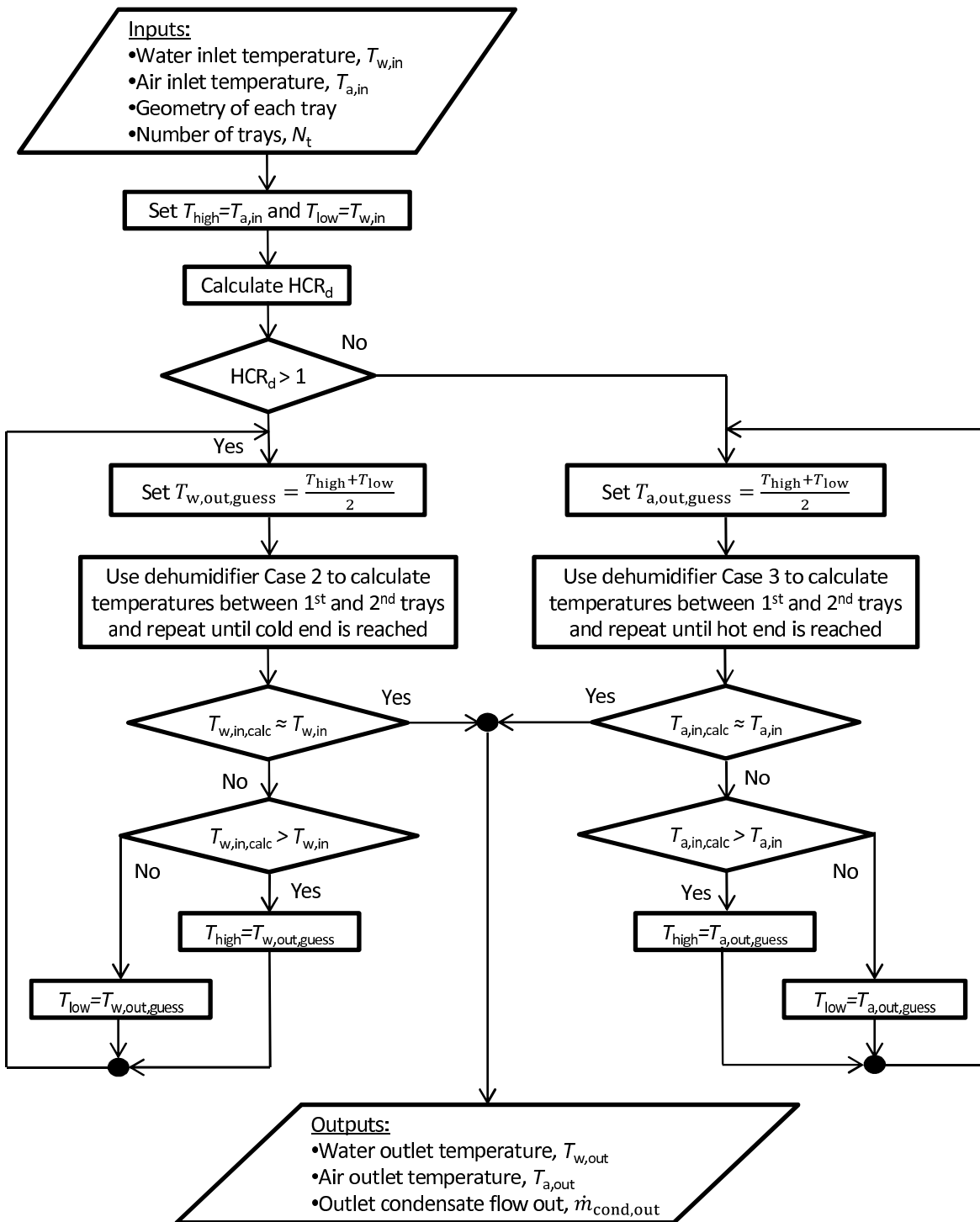


Fig. A.10 Solution algorithm for the multi-tray bubble column dehumidifier.